

Ab Initio Molecular Dynamics Simulations of an Excited State of $X^-(H_2O)_3$ ($X = Cl, I$) Complex

M. Kolaski,^{†,§} Han Myoung Lee, Chaeo Pak, M. Dupuis,[‡] and Kwang S. Kim*

National Creative Research Initiative Center for Superfunctional Materials and Department of Chemistry, Division of Molecular and Life Sciences, Pohang University of Science and Technology, San 31, Hyojadong, Namgu, Pohang, 790-784, Korea, and Molecular Interactions and Transformations, Chemical Sciences Division, Pacific Northwest National Laboratory, K1-83, P.O. Box 999, 906 Battelle Boulevard, Richland, WA 99352

Received: March 11, 2005; In Final Form: August 24, 2005

Upon excitation of $Cl^-(H_2O)_3$ and $I^-(H_2O)_3$ clusters, the electron transfers from the anionic precursor to the solvent, and then the excess electron is stabilized by polar solvent molecules. This process has been investigated using ab initio molecular dynamics (AIMD) simulations of excited states of $Cl^-(H_2O)_3$ and $I^-(H_2O)_3$ clusters. The AIMD simulation results of $Cl^-(H_2O)_3$ and $I^-(H_2O)_3$ are compared, and they are found to be similar. Because the role of the halogen atom in the photoexcitation mechanism is controversial, we also carried out AIMD simulations for the ground-state bare excess electron–water trimer $[e^-(H_2O)_3]$ at 300 K, the results of which are similar to those for the excited state of $X^-(H_2O)_3$ with zero kinetic energy at the initial excitation. This indicates that the rearrangement of the complex is closely related to that of $e^-(H_2O)_3$, whereas the role of the halide anion is not as important.

1. Introduction

The nanoscopic details of ion–water cluster interactions^{1–3} are of importance for understanding solvation phenomena in chemical processes,^{4–6} for designing ionophores and receptors for biological molecular recognition,^{7,8} and for self-assembling nanomaterials using the interaction forces with ions.^{9,10} Because water is a very efficient absorber in the relaxation process of photochemical reactions, photoexcitation of the halide anion–water clusters is a valuable diagnostic tool for studying the dynamics of an excess electron in water.^{11–20} Small clusters consisting of one halogen atom and a few water molecules provide detailed information on molecular interactions. The interwater H-bond-making and -breaking of iodide–water clusters was investigated using IR spectroscopy.²¹ Serxner et al.²² have reported that $I^-(H_2O)_{n=2-4}$ clusters undergo electron transfer from I^- to the dipole-driven water molecules. Lehr et al.¹ used femtosecond photoelectron spectroscopy to investigate the dynamics of small iodine anion–water clusters. They reported that clusters comprising up to four water molecules undergo a simple population decay and that the iodide anion–water clusters for $n \geq 5$ exhibit more complex dynamics.

Density functional and ab initio calculations for halide anion–water clusters,^{11–14,18} as well as excess-electron–water clusters,²³ have been carried out to determine the minimum-energy structures, ionization potentials (IPs), OH stretch frequencies, and charge-transfer-to-solvent (CTTS) energies. All of these clusters have surface- or near-surface-bound states. A few proposals have been made to explain the mechanism of photoexcitation of these halide anion–water clusters.^{1,24–26} All

of these models are based on the static quantum-chemical picture. Recently, Timerghazin and Peshlherbe²⁷ reported interesting results of ab initio molecular dynamics (AIMD) simulations for the excited $I^-(H_2O)_3$ complex. Because the role of the halogen atom in the photoexcitation mechanism of the complex of halide anion and water clusters is not well understood, we compare the dynamic features of the excited states $Cl^-(H_2O)_3$ and $I^-(H_2O)_3$ with the initial kinetic energy (KE) at 0 K, as well as with that of the ground state of $e^-(H_2O)_3$ with the initial kinetic energy (KE) at 300 K.

2. Computational Details

The electronic structure calculations for an excited state were performed with the complete-active-space self-consistent-field (CASSCF) approach. The active space consisted of four electrons and three orbitals (CAS[4,3]), in an approach similar to that used by Timerghazin and Peshlherbe to study $I^-(H_2O)_3$. As the electron of the halide ion transfers to the water cluster upon excitation, the cluster $X^-(H_2O)_3$ ($X = Cl, I$) forms a neutral halogen atom and a negatively charged dipole-driven water cluster, i.e., electron-bound water clusters. Thus, a reasonably large-sized basis set is required to properly describe the excited state, and diffuse functions are needed for the study of dissociation of anionic species including $e^-(H_2O)_n$; otherwise, the excess electron that should have the diffuse nature¹⁹ could be treated as a pseudo-valence electron, in contrast to reality. Therefore, in the present work, oxygen and hydrogen atoms were treated with the correlation-consistent basis sets aug-cc-pVDZ+(2s2p/2s), where the extra diffuse 2s2p and 2s functions were added to all oxygen and hydrogen atoms to effectively bind the excess electron.²³ Because the aug-cc-pVDZ basis set is not available for iodine, the CRENBL ECP basis set²⁸ was used. This basis set employs relativistic core potentials and an extended valence basis set. For the sake of consistency, the CRENBL ECP basis set was also used for the chlorine atom.

* To whom correspondence should be addressed. E-mail: kim@postech.ac.kr.

[†] Pohang University of Science and Technology.

[‡] Pacific Northwest National Laboratory.

[§] Permanent address: Department of Theoretical Chemistry, Institute of Chemistry, University of Silesia, Szkolna 9, 40-006 Katowice, Poland.

In this way, the comparison between $\text{Cl}^-(\text{H}_2\text{O})_n$ and $\text{I}^-(\text{H}_2\text{O})_n$ can be made more properly without a bias arising from the basis set employed. All calculations were carried out using the HONDO suite of programs.²⁹

For both $\text{I}^-(\text{H}_2\text{O})_3$ and $\text{Cl}^-(\text{H}_2\text{O})_3$ clusters, we carried out 500-fs AIMD simulations with a time step of 0.2 fs. In both cases, the initial structures having the ground-state minimum-energy geometry of $\text{X}^-(\text{H}_2\text{O})_3$ were vertically excited. Given that the experiments were done at very low temperatures, we set the initial KEs of the systems to zero. In another AIMD set, the initial velocities were set according to the Maxwell–Boltzmann distribution at 300 K,³⁰ as in our previous molecular dynamics simulations.³¹ Even though this trajectory with the given initial velocities is only one of the many possible dynamics trajectories, it is overall similar to the zero-KE result, except that the KE involving vibrations is much larger. Thus, this dynamics is not described here. In the case that the interaction potentials are already given in terms of analytic functional form without requiring extensive ab initio calculations at each point, a more rigorous sampling technique for the excited-state dynamics from the work of Schincke et al.³² would be used. Because the present excited-state AIMD simulation requires enormous computing time, it is not possible to do more than one or two trajectories in the present study. Thus, to compare the dynamics of $\text{I}^-(\text{H}_2\text{O})_3$ and $\text{Cl}^-(\text{H}_2\text{O})_3$ with the same conditions (that do not depend on the initial velocities), we analyzed the AIMD simulations with the initial KE of zero for our further discussion. This single trajectory is most likely to represent what would be observed near the peak in the distribution of trajectory results.

As the complex of a halide anion and three water molecules is photoexcited, the neutral halide atom is detached from the complex, leaving the $\text{e}^-(\text{H}_2\text{O})_3$ cluster, which transforms toward a more stable energy conformer. This $\text{e}^-(\text{H}_2\text{O})_3$ cluster gains significant KE, as the excited complex undergoes the transformation toward the more stable dissociated structure. To investigate the dynamics of the pure $\text{e}^-(\text{H}_2\text{O})_3$ cluster, we carried out 500-fs AIMD simulations. The initial velocities were set according to the Maxwell–Boltzmann distribution at both 100 and 300 K. The simulation with the initial KE at 100 K did not show the ring-opening process, and so we report only the result obtained from the simulation with the initial KE at 300 K. Though a single trajectory, it is likely to represent what would be observed near the peak in the distribution of trajectory results and is not a very unlikely event near one of the tails of the distribution.

3. Results and Discussion

The structural changes of $\text{Cl}^-(\text{H}_2\text{O})_3$ (initial KE at 0 K), $\text{I}^-(\text{H}_2\text{O})_3$ (initial KE at 0 K), and $\text{e}^-(\text{H}_2\text{O})_3$ (initial KE at 300 K) from 500-fs AIMD simulation trajectories along with the changes of electron density of the highest occupied molecular orbital (HOMO) are shown in Figure 1. The initial and final geometries after 0 and 500 fs of simulation are in Figure 2, and the KE profiles are in Figure 3. The results of $\text{I}^-(\text{H}_2\text{O})_3$ are similar to those of Timerghazin and Peslherbe,²⁷ and there is no significant difference between ours and theirs.³⁴ Our results indicate that the structural changes of $\text{X}^-(\text{H}_2\text{O})_3$ complexes ($\text{X} = \text{Cl}$ and Br) are overall similar regardless of the identity of X . However, it is easily expected that there would be some differences in time scale for the dynamical rearrangement processes of the two systems.

The analysis of $r(\text{X}\cdots\text{O})$ distances appears interesting. $r(\text{X}\cdots\text{O})$ increases faster in the case of $\text{Cl}^-(\text{H}_2\text{O})_3$ than in the case

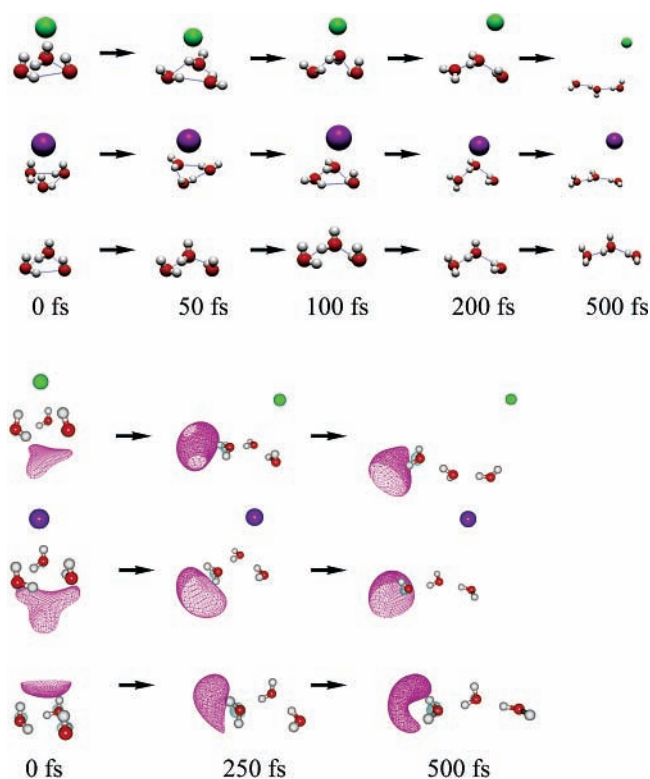


Figure 1. Snapshots of clusters $\text{Cl}^-(\text{H}_2\text{O})_3$ (first), $\text{I}^-(\text{H}_2\text{O})_3$ (second), and $\text{e}^-(\text{H}_2\text{O})_3$ (third line) and the time evolution of the electron density of clusters $\text{Cl}^-(\text{H}_2\text{O})_3$ (fourth), $\text{I}^-(\text{H}_2\text{O})_3$ (fifth), and $\text{e}^-(\text{H}_2\text{O})_3$ (sixth line) taken from AIMD simulations. The hydrogen bonds are drawn using dashed lines. The pictures were drawn using the POSMOL package.³⁶

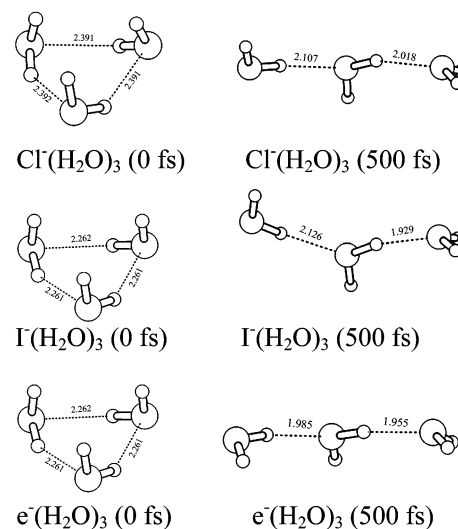


Figure 2. Geometrical parameters of $\text{Cl}^-(\text{H}_2\text{O})_3$, $\text{I}^-(\text{H}_2\text{O})_3$, and $\text{e}^-(\text{H}_2\text{O})_3$ clusters at the initial state and after the 500-fs simulation. The bond lengths are in angstroms.

of the $\text{I}^-(\text{H}_2\text{O})_3$ complex. At the beginning, the separation between the neutral chlorine and the excess-electron-containing water trimer is smaller (~ 3.3 Å) than that between the neutral iodine and the excess-electron-containing water trimer (~ 3.8 Å). Because the dissociation energy of the excited-state $\text{Cl}^-(\text{H}_2\text{O})_3$ is larger than that of the excited-state $\text{I}^-(\text{H}_2\text{O})_3$, the KE of the Cl atom is larger than the KE of the I atom, and thus the Cl atom ejects faster from the cluster. The nearest distance ($\text{X}\cdots\text{O}_3$) from the Cl/I atom to the O atoms of the water molecules changes from 3.3/3.8 Å at 0 fs to 6.4/6.3 Å at 500 fs (Figure 4). Given that the H bond breaks when the interoxygen

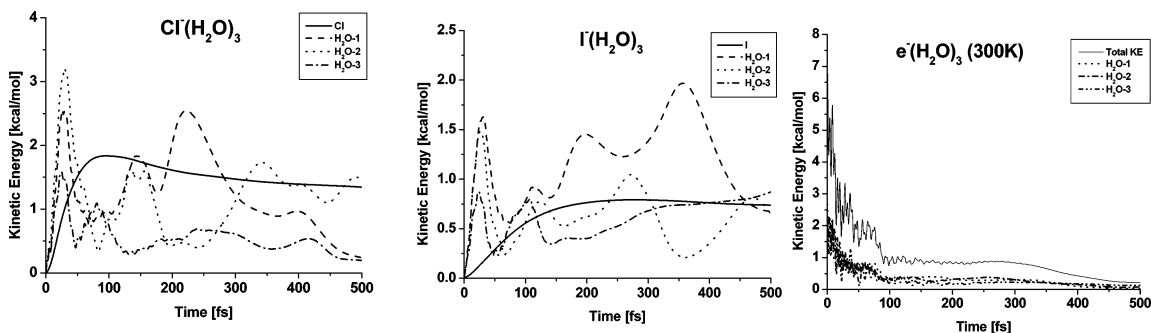


Figure 3. Time evolution of the kinetic energy of the halide and water molecules of $X^-(\text{H}_2\text{O})_3$ clusters.

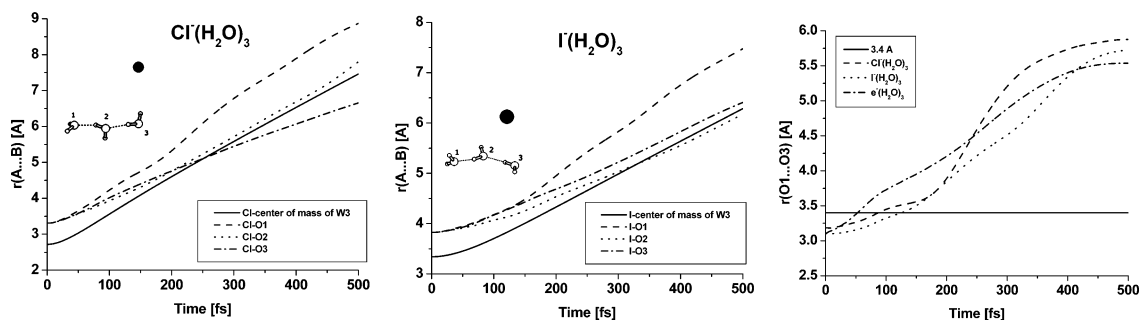


Figure 4. Time evolution of $r(X\cdots\text{O})$ distances and $r(\text{O1}\cdots\text{O3})$ distances for $\text{Cl}^-(\text{H}_2\text{O})_3$, $\text{I}^-(\text{H}_2\text{O})_3$, and $\text{e}^-(\text{H}_2\text{O})_3$ clusters. The solid line represents the time evolution of the distance between the center of mass of the water trimer and the halogen atom.

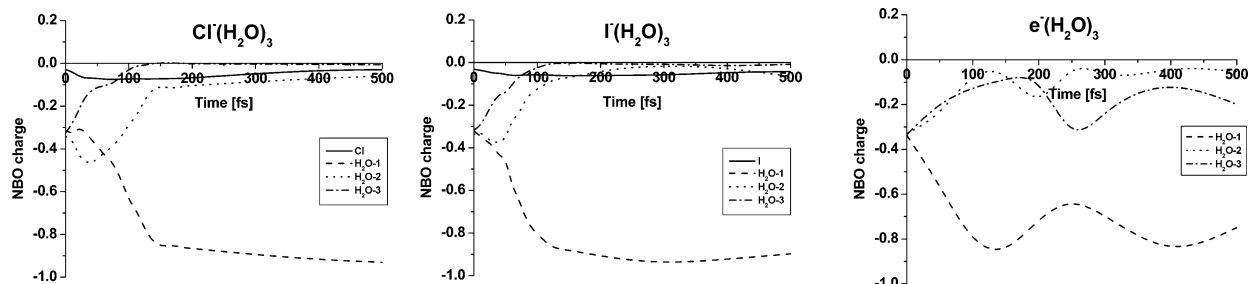


Figure 5. Time evolution of NBO (natural bond orbital) charges localized on the halogen atom and water molecules.

distance is over 3.4 \AA (where the experimental radial distribution function of the liquid water gives the first minimum distinguishing between the first and second solvation shells³³), the ring-opening process occurs at $\sim 100 \text{ fs}$ for $\text{Cl}^-(\text{H}_2\text{O})_3$ and at $\sim 150 \text{ fs}$ for $\text{I}^-(\text{H}_2\text{O})_3$ (Figure 3). In both cases, the ring structure converts to a linear chain. However, given that, at $\sim 150 \text{ fs}$, the $\text{O1}\cdots\text{O3}$ distance for $\text{Cl}^-(\text{H}_2\text{O})_3$ is 3.5 \AA and that for $\text{I}^-(\text{H}_2\text{O})_3$ is 3.4 \AA , the actual difference between the two cases is very small. Thus, the apparent difference is not significant. The velocity of the Cl/I atom with respect to the center of mass (CM) of the water trimer is predicted to be ~ 870 and $\sim 630 \text{ m/s}$, respectively.

Because the excited state of $\text{Cl}^-(\text{H}_2\text{O})_3/\text{I}^-(\text{H}_2\text{O})_3$ at the ground-state geometry upon vertical excitation is not stable, the KE of the chlorine/iodine atom increases very rapidly in the beginning of molecular dynamics simulations and then tends to stay constant (although slightly reduced) after the first 200 fs (Figure 3). The KE profiles of water molecules for both the $\text{Cl}^-(\text{H}_2\text{O})_3$ and $\text{I}^-(\text{H}_2\text{O})_3$ systems are similar. In the beginning of the simulation, the KE of the water cluster increases very rapidly because of the fast reorganization of the water network. At 20 fs, the KE of water cluster is maximized because of the O–H stretch and H-bond stretch modes. This KE is larger for $\text{Cl}^-(\text{H}_2\text{O})_3$ than for $\text{I}^-(\text{H}_2\text{O})_3$ because the dissociation energy of the excited-state $\text{Cl}^-(\text{H}_2\text{O})_3$ on its ground-state-optimum geometry is larger than that of the excited-state $\text{I}^-(\text{H}_2\text{O})_3$ on its

ground-state-optimum geometry. [Vertical excitation energies are 4.7 eV for $\text{Cl}^-(\text{H}_2\text{O})_3$ and 3.6 eV for $\text{I}^-(\text{H}_2\text{O})_3$ on the ground-state-optimized geometry at the CAS[4,3] level; their adiabatic excitation energies are 1.1 eV for $\text{Cl}^-(\text{H}_2\text{O})_3$ and 1.1 eV for $\text{I}^-(\text{H}_2\text{O})_3$; dissociation energies of the excited state on the ground-state optimized geometry are 3.6 eV for $\text{Cl}^-(\text{H}_2\text{O})_3$ and 2.5 eV for $\text{I}^-(\text{H}_2\text{O})_3$.] (Thus, the energy repulsion between the chloride and the water cluster is expected to be larger than that between the iodide and the water cluster.¹⁸) In both cases, after a rapid increase, the KE of the water molecules slightly fluctuates because of the vibrational modes.

We performed an analysis of natural bond orbital (NBO) charges localized on the halogen atom and water molecules (Figure 5). Upon photoexcitation of the $\text{Cl}^-(\text{H}_2\text{O})_3$ and $\text{I}^-(\text{H}_2\text{O})_3$ complexes, the charges of the Cl and I atoms are almost neutral [i.e., only slightly negative (-0.04 au)], and the excess electron is evenly distributed over the whole cyclic water trimer (-0.32 au for each water molecule). As time elapses, the charge distribution gradually changes, and in $\sim 120 \text{ fs}$, the charge is completely redistributed so that the excess electron is almost exclusively on one water molecule ($\text{H}_2\text{O}\text{-1}$, which is located farthest from the X atom in Figure 3) in a large vacant space, while the other two water molecules become almost neutral. The NBO charge of the halogen atom remains constant near zero (although there is a slight change) during the whole run. Thus, the electrostatic repulsion between the near-neutral halide

atom and the electron–water cluster is not important in the dynamics, while the exchange repulsion between the two would give KE (as much as the dissociation energy of the excited state) to the system.

The role of the halogen atom in the rearrangement process of the excess-electron–water cluster has been controversial. Two opposite models have been assumed; one assumes an insignificant role of the halide anion,^{1,24,25} and the other stresses an important role of the halide anion²⁶ in the rearrangement process. To determine whether the halide anion plays an important role in the photoexcitation mechanism, we compared the photodynamics of halide–water clusters with the molecular dynamics of electron–water cluster. We carried out 500-fs ground-state AIMD simulations for the bare excess-electron–water trimer. In this case, the cyclic ring is calculated to be the most stable structure, but it has a negligible small vertical detachment energy (VDE) (0.00–0.01 eV), contrary to the large experimental value (0.13 eV).²³ In the case of the cyclic ring, the excess electron is nearly in the outer large empty space, and so, the excess-electron–water cluster is essentially the same as the neutral water, in consideration of rapid H-tunneling effects.²³ In this regard, the cyclic ring structure of the electron–water trimer can essentially be considered as a system of a free electron and a neutral water trimer. Therefore, it would be more practical to say that the lowest-energy structure for the water trimer binding an excess electron is the linear chain with a VDE of 0.13 eV. In this work, we carried out a ground-state AIMD simulation (by adding initial KE to the atoms according to the Maxwell–Boltzmann distribution at the given temperature) for the system of the cyclic $e^-(\text{H}_2\text{O})_3$ cluster, which imitates the charge-transferred water trimer structure in $X^-(\text{H}_2\text{O})_3$ upon excitation. This ground-state AIMD simulation should be highly dependent on the initial KE or the temperature. At 100 K, the hydrogen bond between water molecules does not break, and the cyclic ring is retained during simulations. At 100 K, the total kinetic energy of the system is too small to convert a cyclic ring into a linear chain. The difference in relative stability between the ring and linear electron–water trimers is around 250 K in the stationary-state study.³⁵ Thus, we carried out a dynamics simulation at 300 K, in which case the ring breaking into linear chain was possible. The NBO charges (Figure 5) and geometry changes (Figures 1, 2, and 4) of $e^-(\text{H}_2\text{O})_3$ in the 300 K simulation are slightly different from, but overall similar to, those of $X^-(\text{H}_2\text{O})_3$ in the excited-state dynamics simulation. In the absence of the halogen atom, the ring breaking into a linear chain occurs at ~ 50 fs. As in the previous cases, all important changes take place at the beginning of the simulations. The important change takes place within ~ 20 fs related to the first period of O–H and H-bond stretch vibrations (Figure 3). Thus, the water O–H stretches play an important role in the initial dynamics. The KEs of the chlorine and iodine atoms show turning points to decrease around 150 and 250 fs, and then the KEs slowly decrease and show convergence (Figure 3). In the absence of the halide atom, the change in NBO charges of the water trimer for the ground-state $e^-(\text{H}_2\text{O})_3$ cluster with the initial KE of 300 K is found to be similar to that of the water trimer for the excited-state $X^-(\text{H}_2\text{O})_3$ cluster with the initial KE at 0 K.

4. Concluding Remarks

In summary, using an approach similar to that employed by Timerghazin and Peslherbe for the study of $\text{I}^-(\text{H}_2\text{O})_3$, we have compared AIMD simulations for both $\text{Cl}^-(\text{H}_2\text{O})_3$ and $\text{I}^-(\text{H}_2\text{O})_3$ clusters. Chlorine and iodine show similar behaviors, but the

dynamics show a slight difference in time scale. We analyzed the time evolution of $r(\text{X}\cdots\text{O})$ distances, kinetic energy terms, and NBO charges. The important changes such as charge distribution and water network organization take place in the beginning of simulations. The role of the halide anion is not important in the rearrangement process of the excess-electron–water cluster. However, the halogen atom plays a certain role in the time scale of the dynamics, possibly because of its mass and the difference in initial kinetic energy arising from the difference in dissociation energy of the excited state at the ground-state-optimal geometry. The excited electron density induces the detachment of the iodide atom and the rearrangement of the solvent because of the stabilization of electron–water cluster. The overall difference in the dynamical rearrangement process between $\text{Cl}^-(\text{H}_2\text{O})_3$ and $\text{I}^-(\text{H}_2\text{O})_3$ is small, except that the Cl atom detaches from the clusters slightly faster than the I atom. These excited-state dynamics of the $X^-(\text{H}_2\text{O})_3$ clusters are similar to the ground-state AIMD features of the bare excess-electron–water trimer at 300 K. Thus, in the rearrangement process of the electron–water cluster in the excited-state of $X^-(\text{H}_2\text{O})_3$, the role of the halide atom is not significant, consistent with the “solvent-driven” model proposed by Neumark¹ and our previous work.²⁴

Acknowledgment. This work was supported by the Creative Research Initiative Project of the Korea Science and Engineering Foundation and Brain Korea 21, and by the Division of Chemical Sciences, Office of Basic Energy Sciences, U.S. Department of Energy.

References and Notes

- (1) (a) Lehr, L.; Zanni, M. T.; Frischkorn, C.; Weinkauff, R.; Neumark, D. M. *Science* **1999**, *284*, 635. (b) Davis, A. V.; Zanni, M. T.; Weinkauff, R.; Neumark, D. M. *Chem. Phys. Lett.* **2002**, *353*, 455.
- (2) (a) Robertson, W. H.; Diken, E. G.; Price, E. A.; Shin, J.-W.; Johnson, M. A. *Science* **2003**, *299*, 1367. (b) Robertson, W. H.; Johnson, W. H. *Science* **2002**, *298*, 69.
- (3) (a) Patwari, G. N.; Lisy, J. M. *J. Chem. Phys.* **2003**, *118*, 8555. (b) Hurley, S. M.; Dermota, T. E.; Hydutsky, D. P.; Castleman, A. W. *Science* **2002**, *298*, 202. (c) Vaden, T. D.; Forinash, B.; Lisy, J. M. *J. Chem. Phys.* **2002**, *117*, 4628. (d) Kim, K. S.; Tarakeshwar, P.; Lee, J. Y. *Chem. Rev.* **2000**, *100*, 4145. (e) Klopfer, J. A.; Vilchiz, V. H.; Lenchenkov, V. A.; Germaine, A. C.; Bradforth, S. E. *J. Chem. Phys.* **2000**, *113*, 6288. (f) Carbacos, O. M.; Weinheimer, C. J.; Lisy, J. M. *J. Chem. Phys.* **1999**, *110*, 8429. (g) Deng, H.; Kebarle, P. *J. Phys. Chem. A* **1998**, *102*, 571. (h) Knipping, E. M.; Lakin, M. J.; Foster, K. L.; Jungwirth, P.; Tobias, D. J.; Gerber, R. B.; Dabdub, D.; Finlayson-Pitts, B. J. *Science* **2000**, *288*, 301. (i) Wang, X.-B.; Yang, X.; Nicholas, J. B.; Wang, L.-S. *Science* **2001**, *294*, 1322.
- (4) (a) Marcus, Y. *Ion Solvation*; Wiley: Chichester, U.K., 1985. (b) Kirk, K. L. *Biochemistry of Halogens and Inorganic Halides*; Plenum Press: New York, 1991. (c) Richens, D. T. *The Chemistry of Aqua Ions*; Wiley: Chichester, U.K., 1997. (d) Lisy, J. M. *Int. Rev. Phys. Chem.* **1997**, *16*, 267. (e) A. W. Castelman, *Adv. Gas-Phase Ion Chem.* **1998**, *3*, 185. (f) Tarakeshwar, P.; Lee, H. M.; Kim, K. S. In *Reviews of Modern Quantum Chemistry*; Sen, K. D., Ed.; World Scientific: Singapore, 2002; pp 1642–1683. (g) Coe, J. V. *Int. Rev. Phys. Chem.* **2001**, *20*, 33.
- (5) (a) Katz, A. K.; Glusker, J. P.; Beebe, S. A.; Bock, C. W. *J. Am. Chem. Soc.* **1996**, *118*, 5752. (b) Jensen, F. *J. Am. Chem. Soc.* **1992**, *114*, 9533. (c) Garmer, D. R.; Krauss, M. *J. Am. Chem. Soc.* **1992**, *114*, 6487. (d) Rodgers, M. T.; Armentrout, P. B. *J. Phys. Chem. A* **1997**, *101*, 1238. (e) Stace, A. J. *Science* **2001**, *294*, 1292.
- (6) (a) Perera, L.; Berkowitz, M. L. *J. Chem. Phys.* **1994**, *100*, 3085. (b) Yeh, I.-C.; Perera, L.; Berkowitz, M. L. *Chem. Phys. Lett.* **1997**, *264*, 31. (c) Feller, D.; Glendening, E. D.; Woon, D. E.; Feyereisen, M. W. *J. Chem. Phys.* **1995**, *103*, 3526. (d) Roeselova, M.; Mucha, M.; Schmidt, B.; Jungwirth, P. *J. Phys. Chem. A* **2002**, *106*, 12229. (e) Gai, H.; Schenter, G. K.; Dang, L. X.; Garrett, B. C. *J. Chem. Phys.* **1996**, *105*, 8835.
- (7) (a) Kwon, J. Y.; Singh, N. J.; Kim, H. N.; Kim, S. K.; Kim, K. S.; Yoon, J. *J. Am. Chem. Soc.* **2004**, *126*, 8892. (b) Yoon, J.; Kim, K. S.; Singh, N. J.; Lee, J. W.; Yang, Y. J.; Kavitha, C.; Kim, K. S. *J. Org. Chem.* **2004**, *69*, 581. (c) Kim, S. K.; Singh, N. J.; Kim, S. J.; Kim, H. G.; Kim, J. K.; Lee, J. W.; Kim, K. S.; Yoon, J. *Org. Lett.* **2003**, *5*, 2083.

- (8) (a) Ihm, H.; Yun, S.; Kim, H. G.; Kim, J. K.; Kim, K. S. *Org. Lett.* **2002**, *4*, 2897. (b) Choi, H. S.; Suh, S. B.; Cho, S. J.; Kim, K. S. *Proc. Natl. Acad. Sci. U.S.A.* **1998**, *95*, 12094.
- (9) Atwood, J. L.; Davis, J. E. D.; MacNicol, D. D.; Vögtle, F.; Lehn, J.-M., Eds. *Comprehensive Supramolecular Chemistry*; Elsevier: Amsterdam, 1996; Vols. 1–11.
- (10) (a) Tarakeshwar, P.; Kim, K. S. Nanorecognition. In *Encyclopedia of Nanoscience and Nanotechnology*; Nalwa, H. S., Ed.; American Scientific Publishers: Stevenson Ranch, CA, 2004; Vol. 7, pp 367–404. (b) Kim, K. S.; Tarakeshwar, P.; Lee, H. M. In *Dekker Encyclopedia of Nanoscience and Nanotechnology*; Schwarz, J. A., Contescu, C., Putyera, K., Eds.; Marcel Dekker: New York, 2004; Vol. 3, pp 2423–2433. (c) Hong, B. H.; Bae, S. C.; Lee, C.-W.; Jeong, S.; Kim, K. S. *Science* **2001**, *294*, 348. (d) Kim, K. S.; Suh, S. B.; Kim, J. C.; Hong, B. H.; Lee, E. C.; Yun, S.; Tarakeshwar, P.; Lee, J. Y.; Kim, Y.; Ihm, H.; Kim, H. G.; Lee, J. W.; Kim, J. K.; Lee, H. M.; Kim, D.; Cui, C.; Youn, S. J.; Chung, H. Y.; Choi, H. S.; Lee, C.-W.; Cho, S. J.; Jeong, S.; Cho, J.-H. *J. Am. Chem. Soc.* **2002**, *124*, 14268.
- (11) (a) Markovich, G.; Giniger, R.; Levin, M.; Cheshnovsky, O. *J. Chem. Phys.* **1991**, *95*, 9416. (b) Kloepfer, J. A.; Vilchiz, V. H.; Lenchenkov, V. A.; Bradforth, S. E. *Chem. Phys. Lett.* **1998**, *298*, 120. (c) Kloepfer, J. A.; Vilchiz, V. H.; Lenchenkov, V. A.; Germaine, A. C.; Bradforth, S. E. *J. Chem. Phys.* **2000**, *113*, 6288.
- (12) (a) Ayotte, P.; Weddle, G. H.; Kim, J.; Kelley, J.; Johnson, M. A. *J. Phys. Chem. A* **1999**, *103*, 443. (b) Ayotte, P.; Weddle, G. H.; Kim, J.; Johnson, M. A. *Chem. Phys.* **1998**, *239*, 485.
- (13) Choi, J.-H.; Kuwata, K. T.; Cao, Y.-B.; Okumura, M. *J. Phys. Chem. A* **1998**, *102*, 503.
- (14) (a) Thompson, W. H.; Hynes, J. T. *J. Am. Chem. Soc.* **2000**, *122*, 6278. (b) Wies, P.; Kemper, P. R.; Bowers, M. T.; Xantheas, S. S. *J. Am. Chem. Soc.* **1999**, *121*, 3531. (c) Cabarcos, O. M.; Weinheimer, C. J.; Lisy, J. M.; Xantheas, S. S. *J. Chem. Phys.* **1999**, *110*, 5.
- (15) Yang, X.; Wang, X.-B.; Wang, L.-S. *J. Chem. Phys.* **2001**, *115*, 2889.
- (16) (a) Borgis, D.; Staib, A. *Chem. Phys. Lett.* **1994**, *230*, 405. (b) Borgis, D.; Staib, A. *J. Chem. Phys.* **1996**, *104*, 4776. (c) Chaudhury, P.; Saha, R.; Bhattacharyya, S. P. *Chem. Phys.* **2001**, *270*, 277. (d) Roszak, S.; Kowal, M.; Góra, R. W.; Leszczyński, J. *J. Chem. Phys.* **2001**, *115*, 3469.
- (17) (a) Lee, E. C.; Lee, H. M.; Tarakeshwar, P.; Kim, K. S. *J. Chem. Phys.* **2003**, *119*, 7725. (b) Lee, H. M.; Tarakeshwar, P.; Park, J.; Kołaski, M. R.; Yoon, Y. J.; Yi, H.-B.; Kim, W. Y.; Kim, K. S. *J. Phys. Chem. A* **2004**, *108*, 2949.
- (18) (a) Baik, J.; Kim, J.; Majumdar, D.; Kim, K. S. *J. Chem. Phys.* **1999**, *110*, 9116. (b) Majumdar, D.; Kim, J.; Kim, K. S. *J. Chem. Phys.* **2000**, *112*, 101. (c) Kim, J.; Lee, H. M.; Suh, S. B.; Majumdar, D.; Kim, K. S. *J. Chem. Phys.* **2000**, *113*, 5259. (d) Lee, H. M.; Kim, K. S. *J. Chem. Phys.* **2001**, *114*, 4461. (e) Lee, H. M.; Kim, D.; Kim, K. S. *J. Chem. Phys.* **2002**, *116*, 5509.
- (19) (a) Kim, J.; Lee, J. Y.; Oh, K. S.; Park, J. M.; Lee, S.; Kim, K. S. *Phys. Rev. A* **1999**, *59*, R930. (b) Kim, J.; Suh, S. B.; Kim, K. S. *J. Chem. Phys.* **1999**, *111*, 10077. (c) Suh, S. B.; Lee, H. M.; Kim, J.; Lee, J. Y.; Kim, K. S. *J. Chem. Phys.* **2000**, *113*, 5273.
- (20) (a) Re, S.; Osamura, Y.; Suzuki, Y.; Schaefer, H. F., III. *J. Chem. Phys.* **1998**, *109*, 973. (b) Al-Halabi, A. S.; Bianco, R.; Hynes, J. T. *J. Phys. Chem. A* **2002**, *106*, 7639. (c) Wei, D.; Truchon, J.-F.; Sirois, S.; Salahub, D. *J. Chem. Phys.* **2002**, *116*, 6028. (d) Odde, S.; Mhin, B. J.; Lee, S.; Lee, H. M.; Kim, K. S. *J. Chem. Phys.* **2004**, *120*, 9524. (e) Park, J.; Kołaski, M.; Lee, H. M.; Kim, K. S. *J. Chem. Phys.* **2004**, *121*, 3106. (f) Odde, S.; Park, C.; Lee, H. M.; Kim, K. S.; Mhin, B. J. *J. Chem. Phys.* **2004**, *121*, 104.
- (21) Ayotte, P.; Weddle, G. H.; Kim, J.; Johnson, M. A. *Chem. Phys.* **1998**, *239*, 485.
- (22) Serxner, D.; Dessent, C. E.; Johnson, M. A. *J. Chem. Phys.* **1996**, *105*, 7231.
- (23) (a) Lee, H. M.; Lee, S.; Kim, K. S. *J. Chem. Phys.* **2003**, *119*, 187. (b) Lee, H. M.; Suh, S. B.; and Kim, K. S. *J. Chem. Phys.* **2003**, *118*, 9981. (c) Lee, H. M.; Kim, K. S. *J. Chem. Phys.* **2002**, *117*, 706. (d) Lee, H. M.; Suh, S. B.; Tarakeshwar, P.; Kim, K. S. *J. Chem. Phys.* **2005**, *122*, 044309.
- (24) Lee, H. M.; Suh, S. B.; Kim, K. S. *J. Chem. Phys.* **2003**, *119*, 007685.
- (25) Vila, F. D.; Jordan, K. D. *J. Phys. Chem. A* **2002**, *106*, 1391.
- (26) (a) Chen, H.-Y.; Sheu, W.-S. *J. Am. Chem. Soc.* **2000**, *122*, 7534. (b) Chen, H.-Y.; Sheu, W.-S. *Chem. Phys. Lett.* **2001**, *335*, 475. (c) Chen, H.-Y.; Sheu, W.-S. *Chem. Phys. Lett.* **2002**, *353*, 459.
- (27) Timerghazin, Q. K.; Peshlherbe, G. H. *J. Am. Chem. Soc.* **2003**, *125*, 9904.
- (28) Basis sets were obtained from the Extensible Computational Chemistry Environment Basis Set Database, developed and distributed by the Molecular Science Computing Facility, Environmental and Molecular Sciences Laboratory, Pacific Northwest Laboratory, P.O. Box 999, Richland, WA 99352 (<http://www.emsl.pnl.gov>).
- (29) Dupuis, M.; Marquez, A.; Davidson, E. R. *HONDO 99.6*, 1999, based on *HONDO 95.3*, by Dupuis, M.; Marquez, A.; Davidson, E. R. Quantum Chemistry Program Exchange (QCPE), Indiana University, Bloomington, IN 47405.
- (30) Case, D. A.; Darden, T. A.; Chetham, T. E.; Simmerling, C. L.; Wang, J.; Duke, R. E.; Luo, R.; Merz, K. M.; Wang, B.; Peralman, D. A.; Crowley, M.; Brozell, S.; Tsui, V.; Gohlke, H.; Mongan, J.; Hornak, V.; Cui, G.; Beroza, P.; Schafmeister, C.; Caldwell, J. W.; Ross, W. S.; Kollman, P. A. *AMBER 8 Users' Manual*; University of California: San Francisco, CA, 2004.
- (31) (a) Kim, K. S.; Kim, Nguyen, H. L.; Swaminathan, P. K.; Clementi, E. *J. Phys. Chem.* 1985, *89*, 2870. (b) Choi, H. S.; Suh, S. B.; Cho, S. J.; Kim, K. S. *Proc. Natl. Acad. Sci. U.S.A.* **1998**, *95*, 12094. (c) Suh, S. B.; Cui, C.; Son, H. S.; U, J. S.; Won, Y.; Kim, K. S. *J. Phys. Chem. B* **2002**, *106*, 2061.
- (32) (a) Joyeux, M.; Farantos, S. C.; Schinke, R. *J. Phys. Chem. A* **2002**, *106*, 5407. (b) Yeh, K.-L.; Xie, D.; Zhang, D. H.; Lee, S.-Y.; Schinke, R. *J. Phys. Chem. A* **2003**, *107*, 7215.
- (33) (a) Soper, A. K. *Chem. Phys.* **2000**, *258*, 121. (b) Soper, A. K.; Philips, M. G. *Chem. Phys.* **1986**, *107*, 47. (c) Kim, K. S. *Chem. Phys. Lett.* **1989**, *156*, 261. (d) Sharp, K. A.; Madan, B.; Manas, E.; Vanderkooi, J. M. *J. Chem. Phys.* **2001**, *114*, 1791.
- (34) To compare Cl⁻(H₂O)₃, I⁻(H₂O)₃, and e⁻(H₂O)₃, we intentionally used the same approach as Timerghazin and Peshlherbe,²⁷ who studied I⁻(H₂O)₃ using CAS[4,3] molecular dynamic calculations. However, they used somewhat small basis sets, namely, 6-31+G(d,p) for water and modified LANL2DZ for iodine, and diffuse functions only on the dangling H atoms (H_d) (but not on the H-bonded H atoms). In this biased case, the H bond and e⁻⋯H_d are treated differently, so the H-bond breaking would be slightly delayed. We used a larger basis set, aug-cc-pVDZ+(2s2p/2s), to better describe the excited states and used nonbiased diffuse functions for all atoms to properly treat the excess electron. Instead of their long time step (0.3 fs), we used a shorter time step of 0.2 fs to describe more accurate dynamics (without serious artificial repulsive forces for the H atom near the OH hard-well region in the case of a large time scale). However, our results are overall similar to theirs.
- (35) Lee, S.; Lee, H. M. *Bull. Korean Chem. Soc.* **2003**, *24*, 802.
- (36) Lee, S. J.; Chung, H. Y.; Kim, K. S. *Bull. Korean Chem. Soc.* **2004**, *25*, 1061.